

STRONG [Fe II] EMISSION FROM NGC 1275

RICHARD J. RUDY,¹ ROSS D. COHEN,² GEORGE S. ROSSANO,¹ PETER ERWIN,¹ R. C. PUETTER,^{1,2}
MATTHEW A. GREENHOUSE,³ AND CHARLES E. WOODWARD⁴*Received 1992 August 17; accepted 1993 March 22*

ABSTRACT

Infrared spectroscopy of the central region of NGC 1275 has revealed an unusually strong [Fe II] $\lambda 12567$ feature. Although the redshift of this line matches those of the lines of the active nucleus, its much narrower profile signifies its origin in a different volume of gas. The strength of the [Fe II] feature compared to the other emission lines from the central region indicates that iron remains relatively undepleted from the interstellar medium of NGC 1275. While other agents may contribute to the [Fe II] emission, we propose that the bulk of the emission is excited by wide-spread shocks. These shocks enrich the iron content of the interstellar medium, excite the extensive low-ionization regions which produce the [Fe II] flux, and contribute to the other low-excitation features which are so distinctive in the spectrum of NGC 1275. These shocks could result from supernova explosions, the accretion on intracluster material, galaxy-galaxy interactions, or some process associated with the active nucleus, but our observations do not distinguish among these phenomena. However, if supernovae generate the shocks, then a very high, and observable, supernovae rate of $\sim 3 \text{ yr}^{-1}$ is implied by the [Fe II] luminosity.

The presence of an [Fe II] feature comparable in brightness to the nuclear Pa β emission, but exhibiting a very different profile, makes NGC 1275 an unambiguous example of a luminous active galaxy where the [Fe II] emission does not originate in the active nucleus, and probably is not powered by the nuclear continuum source. While this observation of NGC 1275 does not exclude the active nucleus as the principal source of the strong [Fe II] emission detected in other active galaxies, it does indicate that other agents (e.g., shocks) can compete favorably in the production of the [Fe II] lines.

Subject headings: galaxies: individual (NGC 1275) — galaxies: ISM — galaxies: nuclei — galaxies: Seyfert — infrared: galaxies — shock waves

1. INTRODUCTION

NGC 1275 is the dominant elliptical galaxy of the Perseus cluster. It harbors an intense radio source (3C 84) and a nucleus which is the source of Seyfert-like emission lines. Branching out from the nucleus and extending several kiloparsecs is a filigree of emission-line regions (Lynds 1970). Much observational work has focused on these and other off-nuclear regions. The emission lines from these regions group into two distinct velocity systems: a so-called low-velocity (LV) system (which is the principal focus of this paper) with the galaxian and nuclear redshift of $\sim 5300 \text{ km s}^{-1}$, and a high-velocity (HV) system with a recessional velocity of $\sim 8200 \text{ km s}^{-1}$. The extranuclear component of the low-velocity system, which encompasses most of the emission-line filaments, probably results from the cooling flows produced by the accretion of intracluster material (Romanishin 1987; Lazareff et al. 1989; Heckman et al. 1989). The lines from this system have FWHM $\sim 350 \text{ km s}^{-1}$ (Kent & Sargent 1979) and the emission is centered on the nucleus. The high-velocity system is concentrated to the northwest of the nucleus (Unger et al. 1990), and displays emission lines characteristic of a giant H II region with profiles

narrower than those of the LV system (Kent & Sargent 1979). Absorption of the nuclear radio continuum by neutral gas in the HV system (De Young, Roberts, & Saslaw 1973), and absorption of the nuclear continuum at the wavelength corresponding to Ly α (Briggs, Snijders, & Bokserberg 1982) indicate that part of the HV system lies between the nucleus of NGC 1275 and Earth. Imaging in the light of emission lines suggests that the HV system is interacting with NGC 1275 (Unger et al. 1990), and the recent detection of stars in the HV system (Boroson 1990) has lent support to the notion originally suggested by Baade & Minkowski (1954) that it is actually an infalling galaxy.

In the course of our program of near-IR spectroscopy of active and star-forming galaxies, we have identified strong [Fe II] $\lambda 12567$ emission from the low-velocity system of NGC 1275. In this paper we report these observations, together with additional infrared data and complementary optical spectrophotometry of the central region of NGC 1275. We use these measurements to investigate conditions within the low-velocity system, and we discuss the implications of these observations of NGC 1275 for understanding the [Fe II] emission from other active galaxies.

2. OBSERVATIONS

The infrared observations of NGC 1275 were acquired on the nights of 1991 August 2 (UT), 1992 August 17 and 20 (UT), and 1992 October 6 (UT) with the 3 m Shane telescope of Lick Observatory. The spectrometer scans a 600 line mm^{-1} grating to provide wavelength selection. The spectral resolution varies from $\lambda/\Delta\lambda \sim 350$ at $0.95 \mu\text{m}$ to ~ 550 at $1.3 \mu\text{m}$, where $\Delta\lambda$ is the

¹ Space and Environment Technology Center, The Aerospace Corporation, M2/266, P.O. Box 92957, Los Angeles, CA 90009.

² Center for Astrophysics and Space Sciences, University of California, San Diego, C-011, La Jolla, CA 92093.

³ Laboratory for Astrophysics, National Air and Space Museum, Smithsonian Institution, Washington, DC 20560.

⁴ Wyoming Infrared Observatory, University of Wyoming, Laramie, WY 82071.

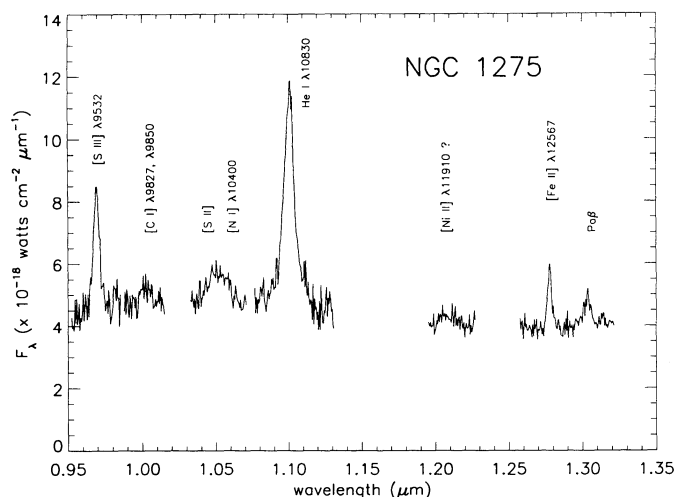


FIG. 1.—Near-infrared spectrum of the nucleus of NGC 1275. Identifications for the prominent emission lines and locations for weaker features are labeled. Relative fluxes for the emission lines are given in Table 1.

measured FWHM of an unresolved feature at the wavelength λ . The spacing between data points was approximately one-fourth of a resolution element. The detector is a germanium photodiode used in conjunction with a charge-integrating amplifier. Sky subtraction was performed by observing sky in an area $\sim 1'$ northwest of the nucleus in a comparatively clear region of the cluster. The aperture is oval in shape with major and minor axes of $9''.6$ and $8''.1$, respectively. The spectrum was divided by that of the comparison star 54 Persei (G8 III) to correct for telluric absorption. The flux calibration of this star is tied to the absolute flux calibration of α Lyr reported by Hayes & Latham (1975; see Rudy et al. 1989 for additional details). The spectral shape for 54 Persei was drawn from the models of Kurucz (1991). The infrared spectrum of NGC 1275 is shown in Figure 1.

The optical data were acquired 1985 October 19 with the Shane 3 m using the image dissector scanner. Observations of the source plus the nearby sky were obtained through both small and large sets of paired, circular apertures. The diameters of the apertures were $2''.8$ and $8''$, respectively. Data from the small aperture measurements are of higher resolution and are presented in Figure 2. Large aperture optical data have been combined with the infrared observations to produce the com-

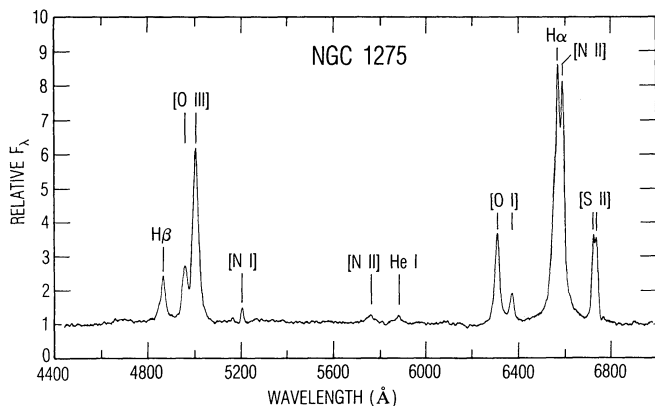


FIG. 2.—Optical spectrum of the central $2''.8$ of NGC 1275

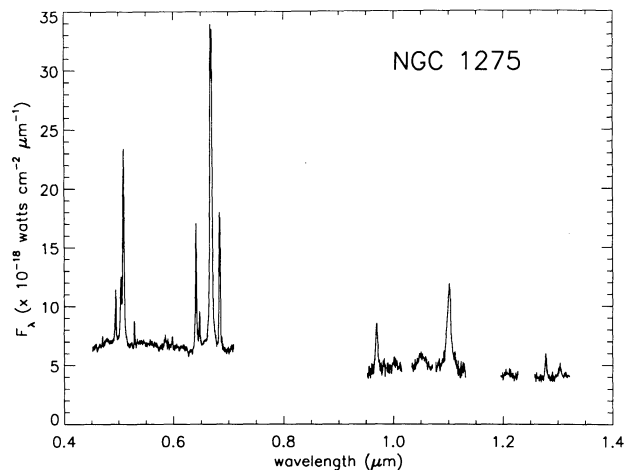


FIG. 3.—A composite optical/near-infrared spectrum of NGC 1275. The optical observations were acquired 6 years earlier than the infrared data. The aperture for the infrared measurements was a $8''.1 \times 9''.6$ oval; the optical aperture was circular and $8''$ in diameter.

posite spectrum of Figure 3. No correction was made for the slight difference between the IR and optical apertures. The ratios of the measured line fluxes relative to $H\beta$ from both apertures are included in Table 1. All optical data were reduced following standard procedures of flat-field correction, wavelength calibration, and flux calibration described in detail by Cohen & Osterbrock (1981).

From previous observations with the IR spectrograph and from observations of the $[Fe II]$ feature which was measured on three of the four nights, we estimate the errors in the relative strengths of the infrared lines to be $\sim 15\%$. The exceptions are the $[C I]$ feature, for which the detection is marginal, $Pa\beta$, for which the S/N is too low to obtain an accurate measure of the flux in the broad wings, and the combination of $[Ni II] \lambda 11910$

TABLE 1
RELATIVE EMISSION-LINE STRENGTHS FOR NGC 1275

ION	$F/F(H\beta)^a$	
	Small	Large
$H\beta \lambda 4861$	1.00	1.00
$[O III] \lambda 4959$	1.13	1.45
$[O III] \lambda 5007$	3.33	4.26
$[N I] \lambda 5199$	0.12	0.28
$[N II] \lambda 5755$	0.18	0.27
$He I \lambda 5876$	0.13	0.17
$[O I] \lambda 6300$	1.43	1.78
$[O I] \lambda 6364$	0.56	0.70
$[N II] \lambda 6548$	0.21	13.1
$H\alpha \lambda 6563$	6.40	
$[N II] \lambda 6583$	2.00	2.65
$[S II] \lambda 6716$	0.67	
$[S II] \lambda 6731$	0.79	
$[S III], Pa\delta \lambda\lambda 9532, 9545$	1.88
$[C I] \lambda\lambda 9823, 9850$	< 0.45
$[S II] \lambda\lambda 10287-10350$	~ 1.20
$[N I] \lambda 10400$	~ 0.64
$He I + Pa\gamma \lambda\lambda 10830, 10938$	5.69
$[Fe II] \lambda 12567$	0.73
$Pa\beta \lambda 12818$	0.50

^a $F(H\beta)$ in $8''$ diameter aperture = 1.3×10^{-13} ergs cm^{-2} s^{-1} .

and [P II] $\lambda 11883$, for which the observations are suggestive but do not confirm a detection. The relative flux in the [S II] auroral lines and [N I] $\lambda 10400$, which are blended, are also uncertain. To separate the two, we compared the shape of the blend in NGC 1275 with observations of the same complex of lines in the planetary nebula NGC 7027 (Rudy et al. 1992). By smoothing the NGC 7027 data to a line width similar to that of the [S II] and [N I] lines of NGC 1275, the relative distribution of flux between the features was estimated.

Both the optical and infrared data were obtained under photometric conditions, and absolute intensities should be accurate to within 25% for each data set. The relative errors between the optical and IR data, however, are uncertain, being subject to source variability in the 6 yr separating the observations. The similar levels of the optical and infrared continua in the composite spectrum (Fig. 3) rule out any large changes. Furthermore, our measured $H\beta$ flux and our value for the [S II] and [N I] complex are identical to the values reported by Wampler (1968). However, our flux for He I $\lambda 10830$ and Pa γ is almost twice the value reported by Rudy et al. (1989), whose infrared observations were concurrent with the optical data reported in this paper. In re-examining the low-resolution data from the 1989 paper we found that the assumed level for the continuum on the blue side of $\lambda 10830$ was $\sim 40\%$ too large due to the presence of the [S II] and [N I] lines. When this is accounted for, the fluxes from the 2 epochs agree within the measurement errors.

3. RESULTS

The principal new data presented in this paper are the infrared observations of the [Fe II] $\lambda 12567$ feature. From these observations, and complementary measurements of additional emission lines, three results follow: (1) the [Fe II] feature does not form in the same gas as do the lines of the AGN; (2) the [Fe II] emission is exceptionally strong; and (3) iron is unusually plentiful in the gas phase. The first of these results is apparent from a comparison of the [Fe II] $\lambda 12567$ profile with those of lines from the active nucleus. The second, which is derived from the large equivalent width of the [Fe II] feature, is almost as obvious. The third follows from a comparison of the iron abundance with that of hydrogen, oxygen, and sulfur. Each of these results is considered below, followed by a discussion of possible mechanisms which might power the [Fe II] emission, and the implications of the high gas-phase iron abundance. However, because the analysis of the [Fe II] line involves comparisons of its flux and profile with those of other infrared and optical lines, we begin first with a discussion of the emission-line spectrum from the central region of NGC 1275.

3.1. Spectrum of the Central Region of NGC 1275

The spectrum radiated by the central regions of NGC 1275 defies a simple classification. In addition to obvious AGN (active galactic nucleus) characteristics, there is also evidence for distributed ionization sources (Johnstone & Fabian 1988). These sources include shocks (Fischer et al. 1987; Heckman et al. 1989) and young stars (Shields & Filippenko 1990), and may be linked to the well-known cooling flows present in NGC 1275 (White & Sarazin 1988, and references therein). In this section we use optical and infrared data to highlight differences in the line profiles, densities, and excitation sources indicated by the emission features. These differences illustrate that the spectrum of the central region of NGC 1275 is a mixture of

several component spectra. These components arise from different regions, with different temperatures and densities, and are excited by multiple mechanisms—all points which are helpful in understanding the origin of the [Fe II] emission.

To illustrate the multicomponent nature of the spectrum, we list, in Table 2, line ratios from our data which can distinguish among the various mechanisms that excite bright emission lines in galaxies (Osterbrock 1989). All the lines have been corrected for reddening of $E(B-V) = 0.50$. This reddening is a weighted average of the following values: $E(B-V) = 0.46$ derived from the ratio of the flux of [S II] transauroral lines measured by Wampler (1968) to that of the auroral lines reported here; $E(B-V) = 0.43$ obtained by Malkan (1983) from [O II] and [S II] measurements; $E(B-V) = 0.68$ determined from our $H\alpha/H\beta$ ratio by assuming an intrinsic value of 3.10 (a ratio characteristic of the narrow-line regions of active galaxies [Gaskell 1982; Gaskell & Ferland 1984]); and $E(B-V) = 0.41$ determined from our Pa $\beta/H\beta$ value assuming case B conditions for 10^4 K and $N_e = 10^4$ cm $^{-3}$. For all cases the applicability of the reddening law of Savage & Mathis (1979) was assumed.

In a plot of [N II]/ $H\alpha$ versus [O III]/ $H\beta$, the line ratios of NGC 1275 place it at the boundary between AGN narrow-line regions and H II regions (Osterbrock 1989). This is also true of its location in a [S II]/ $H\alpha$ versus [O III]/ $H\beta$ diagram. Conversely, its position in a [O I]/ $H\alpha$ versus [O III]/ $H\beta$ plot falls well within the region occupied by AGNs. Of the four criteria listed by Osterbrock (1989) which characterize a low-ionization nuclear emission-line region (LINER), the small-aperture line ratios of NGC 1275 meet two ([O I]/ $H\alpha > 0.05$ and [N II] $\lambda 6583/H\alpha < 0.5$), but fail to satisfy the remainder ([O III] $\lambda 5007/H\beta$ in NGC 1275 is greater than 3, [S II] $\lambda 6716 + \lambda 6731$ does not exceed 0.4 of $H\alpha$).

In addition to indicating differing excitation mechanisms, the emission lines of NGC 1275 also yield divergent values for the electron density. For example, the density derived from the [N II] lines is ~ 100 times greater than the value indicated by the [S II] features. The [N II] $\lambda 5755/(\lambda 6545 + \lambda 6483)$ ratio increases with density and its value in NGC 1275 is unusually large. While $\lambda 5755$ is frequently detected in Seyfert galaxies (e.g., Koski 1978; Cohen 1983) its strength relative to [N II] $\lambda 6548$ and $\lambda 6585$ is almost always less than 0.04, and is normally less than 0.02. In NGC 1275 the reddening corrected value is 0.15. This implies that the smallest possible value of N_e exceeds 10^4 cm $^{-3}$ and for $T_e < 15,000$ K, $N_e > 10^5$ cm $^{-3}$. This result is in obvious conflict with the observed ratio of the [S II] lines $\lambda 6716$ and $\lambda 6731$ which implies a much smaller densities ($900\text{--}1400$ cm $^{-3}$) for a broad range of temperatures (5000–15,000 K). This disparity in the densities derived from the [N II] and [S II] lines can be understood by considering the difference in the line profiles. The [S II] lines are narrower than $\lambda 5755$ (see

TABLE 2
DIAGNOSTIC EMISSION-LINE RATIOS

Line Ratio	Value ^{a,b}
{[O III] $\lambda 5007$ }/ $H\beta$	3.12
{[O I] $\lambda 6300$ }/ $H\alpha$	0.23
[N II] $\lambda 6583$ }/ $H\alpha$	0.31
{[S II] $\lambda 6716 + \lambda 6731$ }/ $H\alpha$	0.22

^a Corrected for $E(B-V) = 0.50$.

^b In 2'' diameter aperture.

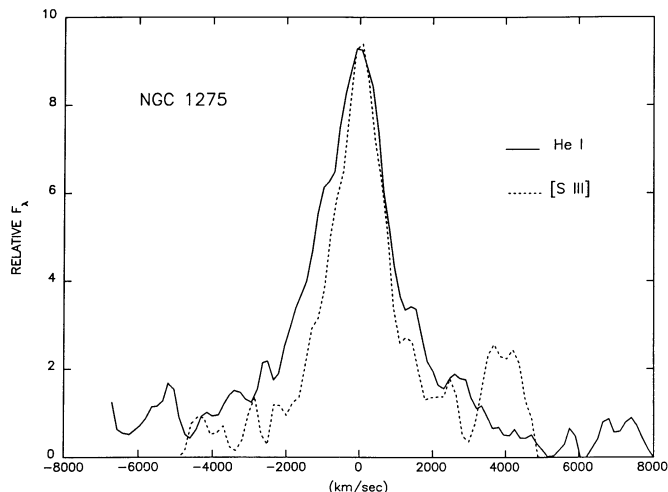


FIG. 4.—A comparison of the line profile of [S III] $\lambda 9532$ with that of He I $\lambda 10830$.

Fig. 2), presumably because much of the [S II] emission arises further from the nucleus. The more distant regions may have very different densities than their more centrally located counterparts.

3.2. [Fe II] $\lambda 12567$ Profile

The two characteristics of the [Fe II] $\lambda 12567$ line which distinguish it with respect to the other emission lines exhibiting the ~ 5300 km s $^{-1}$ redshift are its unusual strength and its narrow profile. In the next section we discuss the intensity of the feature; in this section we compare its profile with those of lines from the active nucleus to demonstrate that the [Fe II] emission and the nuclear lines arise in largely distinct volumes of gas.

Figures 4 and 5 illustrate the very different profile of [Fe II] $\lambda 12567$ with respect to those of the Seyfert lines He I $\lambda 10830$ and [S III] $\lambda 9532$. In Figure 4, He I $\lambda 10830$ and [S III] show the variations in profile width typically exhibited by lines with

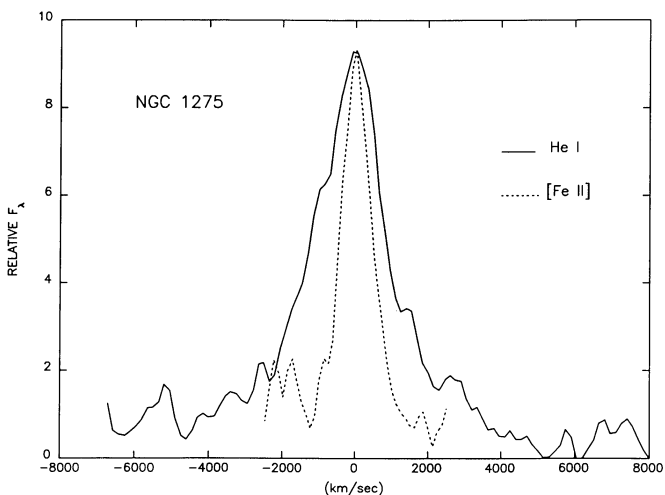


FIG. 5.—A comparison of the line profile of [Fe II] $\lambda 12567$ with that of He I $\lambda 10830$. The observed profile is broadened by the instrumental resolution from an intrinsic value of ~ 730 km s $^{-1}$ to the value of 910 km s $^{-1}$ shown.

different excitation levels and critical densities. He I $\lambda 10830$, which is a permitted transition and presumably forms in the densest and most central region of the nucleus, has a FWHM, corrected for instrumental broadening, of 2020 km s $^{-1}$. The FWHM of the forbidden line [S III] $\lambda 9532$ is 1400 km s $^{-1}$. The [Fe II] profile, shown in Figure 5, is very different from either that of $\lambda 10830$ or $\lambda 9532$. The FWHM of [Fe II] $\lambda 12567$ is only 730 km s $^{-1}$. The narrow width of the [Fe II] feature indicates that it arises from a region whose kinematics are much different than those of the Seyfert nucleus. This difference between the profiles is in distinct contrast with the lines of the Seyfert galaxies NGC 4151 and NGC 1068 (Rieke & Lebofsky 1981; Olivia & Moorwood 1990). Both of these galaxies exhibit strong [Fe II] emission, and in both, the [Fe II] lines have the broad profiles characteristic of an AGN “narrow-line region.” While there are admittedly few published data on near-IR line profiles from active galaxies, observations of NGC 1068 and NGC 4151 being the primary examples, we have surveyed an additional six Seyfert 2 galaxies (Rudy et al. unpublished) and find NGC 1275 to be the only one in which the [Fe II] profile differs radically from lines formed in the active nucleus. The distinctly narrower [Fe II] profile of NGC 1275 underscores the fact that the [Fe II] emission in NGC 1275 originates in a different region than it does in most of its Seyfert counterparts, apparently at the boundaries of, or outside of the active nucleus.

The only other line in our data with a profile as narrow as that of [Fe II] $\lambda 12567$ is [N I] $\lambda 5199$, and the manner in which its intensity varies with aperture size clearly indicates its extranuclear origin. The ratio of $\lambda 5199$ to H β is 2.3 times larger in the $8''$ aperture than in the $2''.8$ aperture, the most pronounced increase with aperture size of any line in our optical data. Moreover, in the observations of Kennicutt (1992), obtained with a $75'' \times 60''$ aperture, [N I] $\lambda 5199$ approaches the strength of H β . Although we do not have multi-aperture observations of [Fe II] $\lambda 12567$, the similar width of its profile to that of [N I] $\lambda 5199$ reinforces the notion that its origin, like that of $\lambda 5199$, is largely extranuclear.

3.3. Intensity of [Fe II] $\lambda 12567$

The second distinctive characteristic of [Fe II] $\lambda 12567$ is its exceptional strength. The [Fe II] $\lambda 12567$ /Pa β value of NGC 1275 is ~ 1.5 , roughly two orders of magnitude greater than the typical value for galactic H II regions and planetary nebulae. For example, the ratios for the Orion nebula and the planetary nebula NGC 7027 are 0.013 and 0.010, respectively (Lowe, Moorhead, & Wehlau 1979; Rudy et al. 1992). Furthermore, the $\lambda 12567$ /Pa β ratio of NGC 1275 is comparable to or greater than the ratios measured directly, or inferred from the [Fe II] $\lambda 16440$ /Br γ ratio, in most AGNs and star-forming galaxies in which [Fe II] emission has been detected (Moorwood & Oliva 1988; Greenhouse et al. 1991). Also, because much of the Pa β flux in NGC 1275 arises within the active nucleus the [Fe II]/Pa β value outside the nucleus where the [Fe II] forms must be even greater than the value we measure. In the next section we discuss one of the reasons for the exceptional intensity of $\lambda 12567$.

3.4. Abundance of Iron in the Gas Phase

Given that the [Fe II] $\lambda 12567$ forms outside of the Seyfert nucleus and that its intensity relative to Pa β is unusually large; we now consider the cause of its exceptional intensity. We

believe that a plentiful supply of iron in the gas phase is at least partially responsible. The importance of this point vis-a-vis the [Fe II] emission is that the depletion of iron from the gas phase due to incorporation into grains frequently limits the intensity of [Fe II] emission. This depletion is normally severe. Depletion factors as great as ~ 1000 , for example, are seen in the interstellar medium (Spitzer & Jenkins 1975; Phillips, Gondhalekar, & Pettini 1982; Pwa & Pottasch 1986). Since direct enrichment mechanisms are believed to be much smaller (iron might be enriched by a factor of ~ 10 in a supernova explosion [Woosley & Weaver 1985]), the gas-phase iron abundance is determined principally by the degree of depletion.

To demonstrate that iron is comparatively undepleted in the central regions of NGC 1275, we compute its abundance relative to sulfur, nitrogen, oxygen, and hydrogen. The abundance ratios are derived using [Fe II] $\lambda 12567$, [S II] $\lambda 6716$, $\lambda 6731$, and the near-infrared auroral lines, [N I] $\lambda 5199$ and $\lambda 10400$, [O I] $\lambda 6300$, and Pa β . We have chosen to use the [S II] and [N I] lines since they form under similar conditions as does $\lambda 12567$. Both S^+ and Fe^+ exist over a comparable range of energies (7.87–16.18 eV for Fe^+ , 10.34–23.4 eV for S^+), and all three ions can exist where hydrogen is neutral. We combine the results for [O I] $\lambda 6300$ and Pa β to yield the ratio of Fe^+ to $(H^0 + H^+)$. Pa β samples the regions where the hydrogen is ionized while $\lambda 6300$ represents the areas where hydrogen is mostly neutral. Because hydrogen and oxygen have virtually identical ionization potentials and are coupled by strong charge exchange reactions, it follows that when hydrogen is neutral, so is oxygen, and when hydrogen is ionized, oxygen is at least singly ionized.

To calculate the relative abundances from the observed line ratios, we computed level populations for the ions over a range of electron temperatures using a 16 level atom for Fe^+ , and 5 level atoms for S^+ , N^0 , and O^+ . For Fe^+ we employed the transition probabilities of Nussbaumer & Storey (1988) and the collision strengths of Nussbaumer & Storey (1980) and Berrington et al. (1988). For the remaining ions we used the atomic parameters tabulated by Osterbrock (1989) and Mendoza (1983). The densities at the various temperatures were chosen to provide the best match to the observed nebular/auroral line ratios for [S II] and [N I].

The results of these calculations are presented in Table 3. The abundance ratios have been divided by the meteoritic ratios given by Grevesse & Anders (1988) to produce the entries in columns (3), (4), and (5). (We have used the meteoritic iron abundance rather than the solar value because recent studies of the Sun based on Fe^+ [Holweger, Heise, & Hock 1990], and on the iron coronal lines [McKenzie & Feldman 1992] give iron abundances smaller than the values determined previously from Fe^0 , and very close to the meteoritic value.) Table 3 shows that most of the Fe^+ abundance ratios are a significant fraction of the meteoritic values, unlike the case in

the interstellar medium of our own Galaxy. The smallest Fe^+/S^+ ratio occurs at the lowest temperature while the minimum $Fe^+/(H^0 + H^+)$ results at the maximum. In fact, it is unlikely that the electron temperature exceeds 10,000 K since [Fe II] $\lambda 8617$ probably would have been detectable in the spectrum of de Bruyn & Sargent (1978). Lower limits on the temperature are less certain but values below 5000 K require very large densities to excite the [N I] and [S II] auroral lines. Clearly, CCD observations of [Fe II] $\lambda 8617$, to measure the temperature, and measurements of [Fe II] $\lambda 12943$ of higher quality, to determine the density, would be useful. To allow for the uncertainty in density, the abundances were also calculated at identical temperatures to those of column (1) but densities that are a factor of 10 smaller than those listed in column (2). (Such densities are consistent with the measure ratio of [S II] $\lambda 6716/6731$, but are at odds with the large strengths of the [S II] auroral and transauroral features.) For the lower densities, the iron depletion features are less than at the higher densities. In addition, [S II], [O I], and Pa β all have line profiles broader than [Fe II] $\lambda 12567$, indicating that the nucleus contributes preferentially to these features and the iron depletion derived from a comparison with the lines of these ions is overestimated. Thus while the largest depletion factor indicated by Table 3 is ~ 15 , the maximum iron depletion factor in the central region of NGC 1275 consistent with the data is probably no more than a factor of 10, and is likely to be less; much smaller than in the interstellar medium of our Galaxy.

4. DISCUSSION

We now consider some of the possible implications of the strong [Fe II] emission, the rich iron abundance, and the prominence of several low-ionization lines.

4.1. Origin of the Gaseous Iron

The two most likely explanations for the rich concentration of iron in the gas in the central regions of NGC 1275 are (1) that the gas in question could be the dust-free material of the cooling flows, or that (2) the dust grains in the gas could have been processed by shocks, returning the iron entrained in these particles to the gas of the interstellar medium. There are additional possibilities, but we consider them less plausible. These include vaporization of dust grains by the nuclear continuum or sputtering by X-rays from either the active nucleus or the cooling flows. The problem with ascribing the dust destruction to either process involving the nucleus is the large separation of the [Fe II] region from the active nucleus, as indicated by the line profile of [Fe II] $\lambda 12567$. This precludes evaporation of large grains and mitigates effects such as X-ray sputtering and single photon heating. Moreover, strong [Fe II] emission, particularly emission originating outside of the narrow-line region, is not a common property of AGNs. This suggests that some agent other than the active nucleus is responsible for the

TABLE 3
DERIVED Fe^+ ABUNDANCE RATIOS FOR A RANGE OF TEMPERATURES AND DENSITIES

T_e	N_e (cm^{-3}) ^a	$N(Fe^+)/N(S^+)^b$	$N(Fe^+)/N(N^0)^b$	$N(Fe^+)/N(H^0 + H^+)$
5000.....	25000	0.064	0.10	0.99
7500.....	15000	0.17	0.27	0.39
10000.....	10000	0.29	0.48	0.20
12500.....	7500	0.40	0.71	0.12

^a Derived from the ratios of auroral and nebular lines for [S II] and [N I].

^b Divided by the meteoritic abundance ratio.

strength of the [Fe II] emission in NGC 1275. The fact that the effects of the cooling flow are weaker than those of the nuclear continuum in the central regions of NGC 1275 (Donahue & Voit [1991] estimate that the nucleus dominates for the central 2 kpc of NGC 1275) makes it even less likely that the cooling flows destroy the dust.

Of the two principal explanations for the high iron content which were cited above, the cooling flows which channel intra-cluster material into the central regions of NGC 1275 may well be the source of the gas we observe. However, the conditions which destroy dust particles or retard their formation within a cooling flow, namely the high temperatures and low densities Fabian, Nulsen, & Canizares (1982), are no longer present in the gas which gives rise to the [Fe II] emission. If, based on the similarities in the profiles of [N I] λ 5199 and [Fe II] λ 12567, we assume that the same gas produces both the [Fe II] and [N I] emission, we can use the temperatures and densities derived from the ratio of the [N I] lines λ 5199, 10400 to estimate the grain formation time. (The densities derived for various temperatures are nearly identical to the values listed in Table 3.) Following the analysis of Spitzer (1978), we find that even if the temperature were significantly less in the past, grains could still grow to a radius of 0.1 μ m in less than 10^6 yr. Since this is probably much less the age of the flow, and since the gas in cooling flows is rich in iron (Edge & Stewart 1991), some additional mechanism must either inhibit dust formation or destroy the grains after they form.

The remaining agent which can account for the rich iron content of the gas is wide-spread shocks. Shocks are believed to be the dominant mechanism processing grains in the interstellar medium (Draine & Salpeter 1979; Seab & Shull 1983; McKee, Chernoff, & Hollenbach 1984; Seab 1987; Shull & Draine 1987). Moreover, shocks can produce many of the low-ionization features (such as [Fe II]) which are so prominent in the spectrum of NGC 1275 (see discussion below). For these reasons, and those discussed above, we believe that shocks are the most likely cause of the abundant iron in the central regions of NGC 1275. It remains, however, to search for additional evidence of shocks in NGC 1275, and to identify their origin.

4.2. Source Powering the [Fe II] Emission

A high iron content alone is not sufficient to account for the strength of the [Fe II] emission from NGC 1275. In addition, the ionization state of the gas must be favorable so that much of the iron exists as Fe^+ . Since Fe^+ is ionized by photons with energies greater than 16.18 eV, the mechanism which powers the luminous [Fe II] line must produce an extensive emission line region whose ionization is low. It has been noted previously that either photoionization by the nucleus or shock heating could produce the low-ionization, off-nuclear emission of NGC 1275 observed at the systemic redshift (Kent & Sargent 1979). To this must be added a third mechanism: photoionization by the diffuse EUV/X-ray emission generated in the cooling flows. In their models, Donahue & Voit (1991) demonstrated that the spectrum emergent from a region ionized by the emission from a cooling flow is strongly dependent on the column density of that region. A broad range of spectra are possible as the column density varies. To produce the prominent low-ionization features seen in NGC 1275, photoionization by the cooling flows or by the nucleus must result in the deposition of energy within regions of mostly neutral material by absorption of high-energy, penetrating

photons. This produces the warm electrons necessary for the collisional excitation of optical and near-IR forbidden lines. Shocks, on the other hand, provide this collisional excitation directly.

We have no definitive data to exclude any of the above three processes as the source of the [Fe II] emission; however, there are difficulties in understanding how photoionization by either the nucleus or the cooling flows could be the active agent. First, the clear difference in profile of λ 12567 from those of the lines of the active nucleus and the fact that the nuclear continuum cannot readily account for the gas-phase iron argue against photoionization by the nuclear continuum. Second, it is unlikely that the cooling flows excite the [Fe II] emission because of their limited effect in the innermost regions of NGC 1275. As noted above, in their calculation of the relative sizes of the zones of influence of the active nucleus versus that of the cooling flows, Donahue & Voit (1991) estimated that the active nucleus dominated within 1 kpc radius of the galaxy center and the cooling flows outside of this distance. This represents a considerable down-scaling from the 18 kpc value given by Branduardi-Raymont et al. (1981), but still falls largely outside of the region spanned by our aperture. It follows that the cooling flows have an even smaller influence on the [Fe II] lines than the active nucleus. Moreover, the [Fe II] feature in NGC 1275 is a much higher contrast line than is typically observed in cooling flow galaxies (e.g., A1795, Cowie et al 1983; A2597, Crawford et al. 1989), suggesting that some other mechanism excites this line.

This once again leaves shocks as the most likely agent. Evidence for global shocks in NGC 1275 has, in fact, already been found in the form of the strong H_2 emission (Fischer et al. 1987). The CO emission detected by Mirabel, Sanders, & Kazes (1989) might also be energized by shocks. In other astronomical sources, large λ 12567/Pa β ratios also frequently result from shocks (Greenhouse et al 1991). In addition to enriching the iron content of the emission line gas, shocks manifest themselves in this manner because the ionization is often so low that iron exists mostly as Fe^+ while hydrogen is predominantly neutral. That the low-ionization nature of shock-excited gas which is favorable for the production of [Fe II] is supported by a variety of observational and theoretical studies. The empirical data are principally observations of supernova remnants (Oliva, Moorwood, & Danziger 1989 and references therein), which show strong [Fe II] emission as well as prominent features from [N I], [C I], [O I], and [S II] such as those radiated by NGC 1275. In fact, it has been postulated that observations of the near-IR [Fe II] lines in other galaxies provide a direct measure of their supernova remnant content (Greenhouse et al. 1991). Numerous theoretical models of shock-excited regions which confirm the prevalence of low-ionization species include Raymond (1979), Hollenbach & McKee (1989), and Shull & Draine (1987).

To search for additional evidence of shocks in NGC 1275, it is first necessary to consider the possible sources of shocks that might be present in NGC 1275. The most likely candidates are the active nucleus, the cooling flows, supernovae, and perhaps interactions with additional members of the Perseus cluster. Although the observational link between supernova and shocks is well known, the observable signatures of shocks generated by the active nucleus, cooling flows, or galaxy-galaxy interactions are not as well established. In searching for supernova remnants, radio maps of NGC 1275 (Pedlar, Booler, & Davies 1983) are inconclusive as to the supernovae content of the central regions. The intense nuclear source, a radio jet, and

the large distance all made the detection of supernova remnants in the central region of NGC 1275 difficult.

Alternate approaches to searching directly for supernova remnants are to look for the young stars that will engender supernovae, or to look for the supernovae explosions themselves. In fact, the formation of stars in the central region of NGC 1275 is a complex topic which has been studied extensively (e.g., van den Bergh 1977; Fabian, Nulsen, & Canizares 1982; Wirth, Kenyon, & Hunter 1983; Shields & Filippenko 1990). While the exact star formation rate and number of young stars in the central region of NGC 1275 is not known, the consensus seems to be that there is excess of blue light indicating the presence of young stars, but there are both fewer young stars and fewer bright, high-mass stars than is expected if all the gas from the cooling flows were incorporated into stars. One upshot of this is that there will be fewer supernovae. However, from a population synthesis analysis of the central 25" region of NGC 1275, Wirth et al. (1983) concluded that B stars account for $\sim 20\%$ of the optical luminosity, a result which suggest a high supernova rate of $\sim 1 \text{ yr}^{-1}$.

There are, to our knowledge, no reports of direct observations of supernovae in NGC 1275 present in the literature. However, the brilliance of the active nucleus makes the detection of supernovae in the central regions difficult. Optical monitoring of NGC 1275 by Lyutyj (1977) showed variations consistent with nine supernova explosions over a period of ~ 7 yr (see discussion in Wirth et al. 1983), an unusually high supernova rate. An additional estimate of the rate can be derived from the measured [Fe II] luminosity. This is done using the parameters adopted by Moorwood & Oliva (1988), namely an average $\lambda 12567$ luminosity per remnant of $700 L_{\odot}$ with the mean lifetime of a remnant being 10^4 yr. For $H_0 = 75$ and $q_0 = 0.5$ this yields a rate of $\sim 3 \text{ yr}^{-1}$. This is a very large value that should be verifiable using modern CCD cameras or periodic *Hubble Space Telescope* images such as those presented by Holtzman et al. (1992).

4.3. Implications of the NGC 1275 Result for [Fe II] Production in AGNs

The manner in which the [Fe II] emission in active galaxies is produced remains a source of some controversy; specifically whether the emission is excited directly by the nucleus, or by some other agent. Joseph et al. (1987) and Kawara, Nishida, & Taniguchi (1988) concluded shocks are the primary mechanism. Supporting this was the work of Moorwood & Oliva (1988) who acknowledged that the nucleus might play a role, but argued from similarities with star-burst galaxies and from the absence of optical [Fe II] lines that the infrared [Fe II] emission is probably not associated with the narrow-line region. The detection of [Fe II] $\lambda 8617$ in several Seyfert galaxies (Osterbrock, Shaw, & Veilleux 1990) weakened this argument. Mouri et al. (1990) found a correlation between [Fe II]/Br γ versus [O I]/H α for a sample of starburst and Seyfert galaxies indicating a spatial coincidence of the [Fe II] and [O I] regions and suggesting a causal link between the [Fe II] emission and the active nucleus in the latter.

Recent observations of [Fe II] $\lambda 12567$ in NGC 1068 by Oliva & Moorwood (1990) showed a broad profile very similar to that of Pa β which linked the [Fe II] line kinematically to the Seyfert nucleus. Graham, Wright, & Longmore (1990) provided a theoretical understanding of how the nucleus could produce the [Fe II] lines when they argued, from a comparison with photoionization processes in the Crab Nebula, that the power-law continua of active nuclei can excite intense [Fe II]

features. In the course of their work, Graham et al. (1990) attributed the bright [Fe II] emission from NGC 4151 to excitation by the nucleus. However, the [Fe II] $\lambda 12567$ line in NGC 4151, like that in NGC 1068, displays the same broad profile as its Pa β counterpart. As noted above, among the luminous AGNs (NGC 1275, NGC 4151, NGC 1068, NGC 6240 and our unpublished sample of Seyfert 2 galaxies) for which infrared [Fe II] line profiles have been measured, NGC 1275 is the only one in which the $\lambda 12567$ profile differs radically from those of the lines of the NLR. The implication is that, for at least this single galaxy, the nucleus does not produce the [Fe II] emission. We do not know if the agent which does is a byproduct of one, or a combination, of the several peculiar features of NGC 1275 (i.e., its massive cooling flows, active nucleus, probable interaction with an infalling galaxy, or possible star formation). A much larger sample of [Fe II] measurements of active galaxies will be necessary to determine whether NGC 1275 is simply unusual, or unique. Until those measurements are available we can summarize by stating that the observations to date suggest that the nucleus dominates the production of [Fe II] in most active galaxies, but that the results for NGC 1275 indicate that processes in addition to photoionization by the nuclear continuum can produce [Fe II] features of comparable intensity.

5. SUMMARY AND CONCLUSIONS

We have reported the detection of a bright [Fe II] $\lambda 12567$ from the central regions of NGC 1275. The intensity of [Fe II] $\lambda 12567$ relative to that of the other emission lines indicates the presence of a high abundance of iron in the gas phase, while the narrow width of the feature implies an origin outside of the active nucleus. The rich iron content of the gas probably results from the destruction of dust grains.

While a power-law continuum from the nucleus (Graham et al. 1990), or from the cooling flows (Donahue & Voit 1991), could excite the [Fe II] emission, neither offers a likely mechanism for processing the circumnuclear dust grains in NGC 1275. This is not the case for shocks, which can also produce the low-ionization features characteristic of the many of the off-nucleus emission line regions of NGC 1275. These include [N I] $\lambda 5199$ with its narrow profile and large spatial extent, as well as [O I] and [S II], which augment the flux from the active nucleus, contributing to the "composite" appearance of the spectrum of the central region. The source of the shocks remains unknown, but supernovae, the active nucleus, galaxy-galaxy interactions, and the cooling flows are possibilities. If supernovae do power [Fe II] $\lambda 12567$, then the high luminosity of the feature signifies a large (and observable) supernova rate.

While ambiguities remain about many aspects of the [Fe II] emission in NGC 1275, it certainly arises outside of the traditional "narrow-line region" associated with the active nucleus and is probably not powered by the nuclear continuum source. These characteristics distinguish NGC 1275 from the small number of other active galaxies for which measurements of the [Fe II] intensity and profile exists, and illustrate that sources other than the active nucleus can produce intense [Fe II] emission.

We thank J. Burrous and K. Baker, the telescope technicians, for their help in acquiring these data. An anonymous referee made several important suggestions. This work was supported by the Aerospace Sponsored Research program in the Space and Environment Technology Center. R. D. C. acknowledges support from NASA grant NAG 5-1630.

REFERENCES

- Baade, W., & Minkowski, R. 1954, *ApJ*, 129, 215
- Berrington, K. A., Burke, P. G., Hibbert, A., Mohan, M., & Baluja, K. L. 1988, *J. Phys. B*, 21, 339
- Boroson, T. A. 1990, *ApJ*, 360, 465
- Branduardi-Raymont, T., et al. 1981, *ApJ*, 248, 55
- Briggs, S. A., Sniijders, M. A. J., & Boksenberg, A. 1982, *Nature*, 300, 336
- Cohen, R. D. 1983, *ApJ*, 273, 489
- Cohen, R. D., & Osterbrock, D. E. 1981, *ApJ*, 243, 81
- Cowie, L. L., Hu, E. M., Jenkins, E. B., & York, D. G. 1983, *ApJ*, 272, 29
- Crawford, C. S., Arnaud, K. A., Fabian, A. C., & Johnstone, R. M. 1989, *MNRAS*, 236, 277
- de Bruyn, A. G., & Sargent, W. L. W. 1978, *AJ*, 83, 1257
- De Young, D. S., Roberts, M. S., & Saslaw, W. C. 1973, *ApJ*, 185, 809
- Donahue, M., & Voit, G. M. 1991, *ApJ*, 381, 361
- Draine, B. T., & Salpeter, E. E. 1979, *ApJ*, 231, 438
- Edge, A., & Stewart, G. 1991, *MNRAS*, 252, 414
- Fabian, A. C., Nulsen, P. E. J., & Canizares, C. R. 1982, *MNRAS*, 201, 933
- Fischer, J., Geballe, T. R., Smith, H. A., Simon, M., & Storey, J. W. V. 1987, *ApJ*, 320, 667
- Gaskell, C. M. 1982, *PASP*, 94, 891
- Gaskell, C. M., & Ferland, G. J. 1984, *PASP*, 96, 393
- Graham, J. R., Wright, G. S., & Longmore, A. J. 1990, *ApJ*, 352, 172
- Greenhouse, M. A., Woodward, C. E., Thronson, H. A., Jr., Rudy, R. J., Rossano, G. S., Erwin, P., & Puetter, R. C. 1991, *ApJ*, 383, 164
- Grevesse, N., & Anders, E. 1989, in *Cosmic Abundances of Matter*, ed: C. Waddington (New York: AIP), 1
- Hayes, D. S., & Latham, D. W. 1975, *ApJ*, 197, 593
- Heckman, T. M., Baum, S. A., van Breugel, W. J. M., & McCarthy, P. 1989, *ApJ*, 338, 48
- Hollenbach, D. J., & McKee, C. F. 1989, *ApJ*, 324, 306
- Holtzman, J. A., et al. 1992, *AJ*, 103, 691
- Holweger, H., Heise, C., & Kock, M. 1990, *A&A*, 232, 510
- Johnstone, R. M., & Fabian, A. C. 1988, *MNRAS*, 233, 581
- Joseph, R. D., Wright, G. S., Graham, J. R., Gatley, I., & Prestwich, A. H. 1987, in *Proc. 2d IRAS Conf. on Star Formation in Galaxies*, ed. C. J. Lonsdale-Persson (ASA CP-2466), 421
- Kawara, K., Nishida, M., & Taniguchi, Y. 1988, *ApJ*, 328, L41
- Kennicutt, R. C., Jr. 1992, *ApJS*, 79, 255
- Kent, S. M., & Sargent, W. L. W. 1979, *ApJ*, 230, 667
- Koski, A. T. 1978, *ApJ*, 223, 56
- Kurucz, R. L. 1991, in *Precision Photometry: Astrophysics of the Galaxy*, ed. A. G. Davis Philip, A. R., Uggren, & K. A. Janes (Schenectady, NY: L. Davis Press)
- Lazareff, B., Castets, A., Kim, D.-W., & Jura, M. 1989, *ApJ*, 336, L13
- Lowe, R. P., Moorehead, J. M., & Wehlau, W. H. 1979, *ApJ*, 228, 191
- Lynds, C. R. 1970, *ApJ*, 159, L151
- Lyutyj, V. M. 1977, *Soviet Astron.*, 21, 655
- Malkan, M. A. 1983, *ApJL*, 264, L1
- McKee, C. F., Chernoff, D. F., & Hollenbach, D. J. 1984, in *Galactic and Extragalactic Infrared Spectroscopy*, ed. M. F. Kessler & L. P. Phillips (Dordrecht: Reidel), 103
- McKenzie, D. L., & Feldman, U. 1992, *ApJ*, in press
- Mendoza, C. 1983, in *Planetary Nebulae*, ed. D. R. Flower (Dordrecht: Reidel), 143
- Mirabel, I. F., Sanders, D. B., & Kazes, I. 1989, *ApJ*, 340, L19
- Moorwood, A. F. M., & Oliva, E. 1988, *A&A*, 203, 278
- Mouri, H., Nishida, M., Taniguchi, Y., & Kawara, K. 1990, *ApJ*, 360, 55
- Nussbaumer, H., & Storey, P. J. 1980, *A&A*, 89, 308
- . 1988, *A&A*, 193, 327
- Oliva, E., Moorwood, A. F. M., & Danziger, I. J. 1989, *A&A*, 214, 307
- . 1990, *A&A*, 240, 453
- Oliva, E., & Moorwood, A. F. M. 1990, *ApJ*, 348, L5
- Osterbrock, D. E. 1989, *Astrophysics of Gaseous Nebulae and Active Galactic Nuclei* (Mill Valley, CA: Univ. Sci. Books)
- Osterbrock, D. E., Shaw, R. A., & Veilleux, S. 1990, *ApJ*, 352, 561
- Pedlar, A., Booler, R. V., & Davies, R. D. 1983, *MNRAS*, 203, 667
- Phillips, A. P., Gondhalekar, P. M., & Pettini, M. 1982, *MNRAS*, 200, 687
- Pwa, T. H., & Pottasch, S. R. 1986, *A&A*, 164, 116
- Raymond, J. C. 1979, *ApJS*, 39, 1
- Rieke, G. H., & Lebofsky, M. J. 1981, *ApJ*, 250, 87
- Romanishin, W. 1987, *ApJ*, 323, L113
- Rudy, R. J., Cohen, R. D., Rossano, G. S., Puetter, R. C., & Chapman, S. C. 1989, *ApJ*, 341, 120
- Rudy, R. J., Erwin, P., Rossano, G. S., & Puetter, R. C. 1992, *ApJ*, 384, 536
- Rudy, R. J., Rossano, G. S., & Puetter, R. C. 1989, *ApJ*, 346, 799
- Savage, B. D., & Mathis, J. S. 1979, *ARA&A*, 17, 73
- Seab, C. G. 1987, in *Interstellar Processes*, ed. D. J. Hollenbach & H. A. Thronson (Dordrecht: Reidel), 491
- Seab, C. G., & Shull, J. M. 1983, *ApJ*, 275, 652
- Shields, J. C., & Filippenko, A. V. 1990, *ApJ*, 353, L7
- Shull, J. M., & Draine, B. T. 1987, in *Interstellar Processes*, ed. D. J. Hollenbach & H. A. Thronson (Dordrecht: Reidel), 283
- Spitzer, L. 1978, in *Physical Processes in the Interstellar Medium* (New York: Wiley)
- Spitzer, L., & Jenkins, E. B. 1975, *ARA&A*, 13, 133
- Unger, S. W., Taylor, K., Pedlar, A., Ghataure, H., Penston, M. V., & Robinson, A. 1990, *MNRAS*, 242, 33P
- van den Bergh, S. 1977, *Astron. Nach.*, 298, 285
- Wampler, E. J. 1968, *ApJ*, 154, L53
- White, R. E. III, Sarazin, C. L. 1988, *ApJ*, 335, 688
- Wirth, A., Kenyon, S. J., & Hunter, D. A. 1983, *ApJ*, 269, 102
- Woosley, S. E., & Weaver, T. A. 1986, in *Nucleosynthesis and Its Implications on Nuclear and Particle Physics*, ed. J. Audouze & N. Mathieu (Dordrecht: Reidel), 145